Available online at www.sciencedirect.com
SCIENCE DIRECT®
Journal of Organometallic Chemistry 690 (2005) 4319–4329
Journal of Organometallic Chemistry
www.elsevier.com/locate/jorganchem

A quantum chemical study on the mechanism of S-coordinated tetrazole-thiolato formation by the reaction of organic isothiocyanates with metal azido complexes of Pt(II), Pd(II), and Sn

Kunhye Lee, Yong-Joo Kim, Kyoung Koo Baeck *

Department of Chemistry, Kangnung National University, Gangnung, Gangwon-do 210-702, Korea

Received 11 May 2005; received in revised form 24 June 2005; accepted 4 July 2005
Available online 10 August 2005

Abstract

The mechanism of the reaction of isothiocyanates with metal-azido complexes of Pt(II), Pd(II), and Sn as well as hydrazoic acid is studied using the density functional theory method. The relative stability between two possible product isomers (S-coordinated tetrazole-thiolato and N-coordinated tetrazolato complexes) does not directly relate to the experimentally synthesized product. The overall reaction proceeds via three steps. The first step is the approach of the S-atom of the organic isothiocyanate to the central metal atom followed by the nucleophilic attack of the coordinated N-atom of the azido group to the C-atom of the isothiocyanate. The activation barrier of this step is 22–24 kcal mol^{-1}, and the resulting intermediate has the imidoyl azide form. In the second reaction step, electrophilic attack of the terminal N-atom of the azido group to the N-atom of the isothiocyanate transforms the intermediate to the S-coordinated tetrazole-thiolato product with a barrier of about 11 kcal mol^{-1}. The N-coordinated tetrazole could be made from the S-coordinated tetrazole-thiolato complex only after the third step, in which the metal coordination migrates from the S- to the N-atom.

Keywords: S-coordinated tetrazole-thiolato; Metal azido complexes; Isothiocyanates; Hydrazoic acid; Reaction mechanism

1. Introduction

Tetrazoles are an increasingly important functionality, not only as precursors to a variety of nitrogen-containing heterocycles [1] but also as materials with applications in diverse areas such as pharmaceuticals [2], explosives [3], information recording systems [4], and corrosion inhibitors [5]. The main route for the formation of tetrazoles, the reaction of organic azides with nitriles, is relatively well known and has been studied through many experiments [6]. The details of its reaction mechanism are also explained by recent theoretical studies [7].

Metal-azido complexes have long been considered to behave in a manner analogous to organic azides and azide salts [8]. The isothiocyanate group can also be an alternative source of the nitrile (CN) moiety that can be utilized for the synthesis of tetrazoles. As the result, the reaction of organic isothiocyanates with metal-azido complexes is expected to generate a metal complex with tetrazole ligands, which can in turn be an alternative source of tetrazoles. Several studies regarding the dipolar cycloaddition of organic isothiocyanates to the azido ligand of metal complexes have been reported [9–11], but the actual coordination of the tetrazole ligand to the central metal was not clearly identified, except in just a few cases involving the formation of tetrazole-thiolato complexes with a direct tin–sulfur bond [12,13].

* Corresponding author. Tel.: +82 33 640 2307; fax: +82 33 647 1183.
E-mail address: baeck@kangnung.ac.kr (K.K. Baeck).

0022-328X/$ - see front matter © 2005 Elsevier B.V. All rights reserved.
doi:10.1016/j.jorganchem.2005.07.022

Recent experimental works have also confirmed that the reaction of di(azido)bis(phosphine) complexes of Pd(II) and Pt(II) with organic isothiocyanates produces S-coordinated tetrazole-thiolato compounds instead of N-coordinated tetrazoles [14], which is in accord with the previous cases involving Sn [12,13]. It now seems clear that the reaction of isothiocyanates with metal-azido complexes produces S-coordinated tetrazole-thiolato compounds, which is in contrast to the long-held expectation of N-coordinated tetrazolato products [9–11]. Although previous work provided a possible semi-empirical qualitative explanation about the expected reaction products [13], the formation of an S-coordinated product was not explained. This result is hard to explain by either an ionic two-step mechanism [15] or a concerted [2 + 3] addition mechanism [6b,16] applied to the reaction of azides with nitriles.

In addition to the recent confirmation of S-coordinated tetrazole-thiolato products [13,14], the lack of proper explanation as well as the limited experimental and theoretical studies on the reaction mechanism of isothiocyanates with metal-azido complexes are the main motivations of this work. Proper understanding of this reaction is indispensable if it is to be used as an alternative source of tetrazoles. Furthermore, an understanding of this reaction is also expected to provide insight into the mechanisms underlying the formation of a wide range of heterocyclic compounds.

To provide detailed information on the target reaction of alkyl isothiocyanates with metal-azido complexes, we first report the structure and energetic stabilities of all reactants and possible product isomers gained by using an ab initio theoretical method. In the second part, all possible intermediates and transition structures for the reaction of methyl isothiocyanate with hydrazoic acid, the simplest prototype of our target reaction, are presented to provide some basic insights. Finally, the reactions of methyl isothiocyanates with transition metal-azido complexes and the mechanism leading to the formation of S-coordinated tetrazole-thiolato products instead of the N-coordinated tetrazole are explained.

2. Computational methods

The density functional theory (DFT) method with the B3LYP functional [17], as implemented in the Gaussian03 program package [18], was used for the optimization of all stationary and transition structures. The first- and second-row atoms were treated by using the 6-31G(d) all-electron basis sets [19], but only four valence electrons of the main group metal (Sn) and 18 valence electrons of the transition metals (Ni, Pd, and Pt) were explicitly treated, whereas chemically inert core-electrons of the metals were treated by using the effective core potential (ECP) method. To include the majority of relativistic effects caused by the high nuclear charge of the heavy elements, the combination of relativistic ECP of Hay and Wadt with its corresponding valence basis sets, the LanL2DZ sets [20], was employed. For the better description of valence electrons, the valence basis set of LanL2DZ was augmented with one set of diffuse d-type functions with $\varsigma = 0.11344$, 0.07532, 0.065, and 0.05480 for Ni, Pd, Sn, and Pt, respectively. The pure, spherical 5d basis functions were employed in all of the calculations.

The vibrational frequencies of all stationary and transition structures were calculated. All of the stationary structures had only positive vibrational frequencies and the transition structures had only one negative frequency. The zero-point energy correction was

Table 1
The relative stability of *cis*/*trans*-isomers of reactants, $\Delta E_{(cis/trans)R}$,[a] the reaction energy of each product, ΔE_{RXN}, and the relative energy between **III** and **IV** products, ΔE_{Rel},[b] for reactions of an alkyl isothiocyanate, RNCS with a $L_2M(N_3)_2$ (M = Ni(II), Pd(II), Pt(II)), L_3SnN_3, or hydrazoic acid (HN_3)

M	Ni	Pd	Pt	Sn	Sn	H
$L = PH_3$				$L = CH_3$	$L = CH_3$	
$R = CH_2CH_3$				$R = C_6H_5$	$R = CH_3$	
$\Delta E_{(cis/trans)R}$[a]	4.2	3.8	0.9			
E_{RXN}(**I**)[c]	10.3	9.3	10.6	14.2	6.9	5.5
E_{RXN}(**II**)[c]	−17.7	−18.2	−22.6	5.2	−4.1	−3.8
E_{RXN}(**III**)[c]	−56.7	−57.5	−61.6	−8.8	−17.2	−19.7
E_{RXN}(**IV**)[c]	−50.9	−60.6	−60.1	−6.3	−13.9	−11.3
ΔE_{Rel}[b]	5.8	−3.1	1.5	2.5	3.3	8.4
$L = PMe_3$						
$R = CH_2CH_3$						
$\Delta E_{(cis/trans)R}$[a]	8.1	6.0	4.0			
E_{RXN}(**III**)[c]	−56.2	−55.6	−57.8			
E_{RXN}(**IV**)[c]	−45.5	−55.5	−53.9			
ΔE_{Rel}[b]	10.7	−0.1	3.9			

All values are given in kcal mol^{-1}.

[a] The positive sign of $\Delta E_{(cis/trans)R}$ implies that the *trans*-reactant has lower energy than the *cis*-reactant.

[b] The positive sign of ΔE_{Rel} means that the M–N(N_3R)CS product is more stable than the M–SC(N_3)NR product.

[c] The numbers **I**, **II**, **III**, and **IV** represent the isomers shown in Scheme 1.

Table 2
The relative energy, ΔE_{Rel} (kcal mol^{-1}), of complex **IV** with respect to the corresponding complex **III** (Scheme 1)

	R	Ni	Pd	Pt
$L = PH_3$	H	4.8	−4.3	0.2
	CH_3	5.8	−3.1	1.3
	CH_2CH_3	5.8	−3.1	1.5
	$CHCH_2$	5.0	−4.1	0.3
$L = PMe_3$	H	20.9	8.0	8.7
	CH_3	10.5	0.0	3.0
	CH_2CH_3	10.7	−0.1	3.9
	$CHCH_2$	11.7	0.3	5.3
	C_6H_5			2.8

Table 3
Some selected bond lengths (Å) and angles (°) of transition structures, intermediate (IMA), and product isomers with the B3LYP/6-31G* method along the reaction path of isothiomethane with hydrazoic acid, shown in Fig. 1

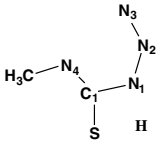	**TS1**	IMA	**TS2**	**IV′**	**TS3**	**III′**	**TS4z**
ΔE	38.6	1.6	14.8	−11.3	21.4	−19.7	26.5
	(39.7)	(3.6)	(18.4)	(−5.8)	(26.6)	(−12.3)	(31.4)
$R(C_1–N_1)$	1.530	1.422	1.421	1.322	1.339	1.370	1.681
	(1.531)	(1.420)	(1.415)	(1.318)	(1.334)	(1.366)	(1.626)
$R(C_1–S)$	1.756	1.801	1.772	1.759	1.723	1.663	1.672
	(1.749)	(1.795)	(1.765)	(1.755)	(1.720)	(1.660)	(1.676)
$R(N_1–H)$	1.202	2.427	2.458	2.651	1.366	1.010	1.017
	(1.198)	(2.422)	(2.458)	(2.639)	(1.347)	(1.008)	(1.015)
R(S–H)	1.826	1.347	1.349	1.348	1.767	3.077	2.777
	(1.813)	(1.342)	(1.344)	(1.344)	(1.760)	(3.065)	(2.741)
$\angle(S–C_1–N_1)$	98.5	110.8	113.8	127.2	108.9	130.2	106.9
	(98.7)	(111.2)	(114.5)	(127.2)	(108.7)	(129.9)	(107.6)
$\angle(C_1–N_1–H)$	87.6	69.4	67.2	59.1	83.6	126.4	117.4
	(86.8)	(69.0)	(66.7)	(59.2)	(83.6)	(126.4)	(117.6)
$\angle(C_1–S–H)$	64.3	94.9	94.8	93.3	62.5	41.3	56.9
	(64.1)	(94.7)	(94.5)	(93.1)	(61.8)	(41.4)	(56.1)
$\angle(N_1–N_2–N_3)$	176.1	172.9	138.8	111.6	108.5	107.2	148.1
	(177.2)	(173.3)	(137.0)	(111.4)	(108.5)	(107.4)	(146.9)
ω_i	−1167		−276		−1652		−302
	(−1159)		(−287)		(−1642)		(−240)
ω_1	68	36	31	72	33	44	69
	(64)	(48)	(37)	(68)	(21)	(57)	(64)

The relative energy ΔE (kcal mol^{-1}) is defined with respect to the separated reactants. The imaginary frequency (ω_i) of transition structures and the lowest vibrational frequency (ω_1) are also given. The results with the B3LYP/6-311++G(2d,p) basis are given in parentheses.

employed in the calculations of relative stability, reaction energy, and activation energy. All the energetic values in Tables 1–4 as well as Figs. 1 and 3 are the values with zero-point correction.

The actual syntheses used dichloromethane as a solvent [14], which is an aprotic solvent and has a relatively small dielectric constant. As the result, the solvent effect was not expected to change any qualitative aspect of the reaction mechanism and thus was not included in the present calculations.

3. Results and discussion

Although several product isomers are possible from the reaction of an isothiocyanate with a metal-azido complex, the relative stabilities of the isomers as well as the reaction energies of each isomer have never been explicitly studied either experimentally or theoretically. Because these quantities are some of the most basic parameters for a qualitative understanding of the reaction, the relative energies of possible isomers and the reaction energy of each isomer are reported in Section 3.1 for the reactions of isothiocyanates with Sn-, Pt(II)-, Pd(II)-, and Ni(II)-azido complexes. Several of the reactions had been carried out previously [13,14].

The reaction mechanism of methyl isothiocynate with hydrazoic acid is reported in Section 3.2 as the simplest prototype of the target reactions described above. This prototype provides insights into the reaction mechanism.

In addition to the reaction mechanisms of methyl isothiocyanate and trimethyl tin azide, the model reactions of methyl isothiocyanate with tris(phosphine) metal-azido cations, for Pt(II) and Pd(II), are reported in Section 3.3. In that section, the reaction mechanism of our target reactions is completely disclosed. A brief description of the reaction of the Ni(II) complex is given in Section 3.4.

3.1. The reaction energy and the relative energy of isomers

The reaction of the metal complexes with organic isothiocyanates, R–NCS, can produce one of three N-coordinated tetrazolato isomers (**I**, **II**, and **III**) or an S-coordinated tetrazole-thiolato compound (**IV**), shown in Scheme 1. The reaction of isothiocyanates with

Table 4
Results for the reaction shown in Fig. 3 with M = Pt

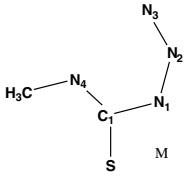

	TS1	IMA	**TS2**	**IV″**	**TS3**	**III″**
ΔE	+22.3	−7.6	+3.3	−24.5	−13.1	−21.9
	(+22.0)	(−8.2)	(+2.3)	(−24.5)	(−15.1)	(−19.1)
	[+23.9]	[+3.7]	[+14.5]	[−13.9]	[−7.7]	[−17.2]
$R(C_1–N_1)$	1.814	1.432	1.440	1.331	1.343	1.368
	(1.854)	(1.432)	(1.440)	(1.332)	(1.346)	(1.366)
	[1.829]	[1.434]	[1.438]	[1.329]	[1.342]	[1.370]
$R(C_1–S)$	1.684	1.811	1.779	1.746	1.721	1.681
	(1.683)	(1.809)	(1.777)	(1.750)	(1.718)	(1.688)
	[1.666]	[1.787]	[1.766]	[1.749]	[1.708]	[1.680]
$R(N_1–M)$	2.121	3.055	3.145	3.397	2.317	2.052
	(2.134)	(2.939)	(2.847)	(3.099)	(2.258)	(2.057)
	[2.146]	[3.131]	[3.025]	[3.191]	[2.344]	[2.125]
R(S–M)	3.136	2.428	2.422	2.420	2.833	3.766
	(3.020)	(2.407)	(2.420)	(2.416)	(2.868)	(3.630)
	[3.336]	[2.484]	[2.502]	[2.513]	[2.903]	[3.737]
$\angle(S–C_1–N_1)$	104.9	111.5	114.1	128.9	119.3	129.1
	(104.2)	(111.0)	(112.5)	(125.7)	(120.8)	(128.0)
	[105.6]	[112.3]	[113.3]	[126.8]	[119.8]	[128.9]
$\angle(C_1–N_1–M)$	113.8	87.9	83.7	72.9	103.7	130.3
	(109.1)	(89.3)	(89.5)	(78.5)	(104.1)	(125.9)
	[119.2]	[87.9]	[87.8]	[79.8]	[104.9]	[127.5]
$\angle(C_1–S–M)$	80.4	102.3	103.0	101.9	76.1	54.8
	(82.2)	(100.0)	(97.3)	(95.6)	(73.6)	(57.2)
	[79.0]	[104.0]	[100.8]	[97.0]	[75.8]	[56.9]
$\angle(N_1–N_2–N_3)$	169.7	173.0	140.9	111.3	109.2	109.4
	(170.8)	(173.1)	(140.4)	(111.0)	(109.3)	(109.3)
	[170.8]	[173.7]	[140.7]	[111.2]	[109.5]	[109.2]
ω_i	−256		−262		−120	
	(−288)		(−260)		(−103)	
	[−230]		[−267]		[−105]	
ω_1	30	19	22	28	30	26
	(22)	(26)	(26)	(26)	(22)	(27)
	[29]	[29]	[15]	[35]	[24]	[32]

The results with M = Pd and Sn are given in parentheses and brackets, respectively. The same units are used as in Table 3.

organotin azides or with hydrazoic acid also can be represented by the same scheme, in which M represents the organotin moiety or an H-atom, respectively.

The reaction energies (E_{RXN}) of four possible product isomers from di(azido)bis(phosphine) complexes of Ni(II), Pd,(II), and Pt(II) are calculated using two phosphine groups (L = PH_3 or PMe_3) on the complex and one alkyl group (R = CH_2CH_3) on the organic isothiocyanates. The reaction of trimethyltin azide (L = CH_3) is studied with either phenyl isothiocyanate (R = C_6H_5) or methyl isothiocyanate (R = CH_3). The reaction of hydrazoic acid with methyl isothiocyanate is also calculated. These results are collated in Table 1 for comparison. The relative stability, ΔE_{Rel}, between N-coordinated tetrazolato (**III**) and S-coordinated tetrazole-thiolato (**IV**) compounds is also emphasized in the table because the two isomers are the most stable and plausible products.

Because the starting reactant, the di(azido)bis(phosphine) metal complex $M\{N_3\}_2\{L\}_2$, has two structural (*cis*- and *trans*-) isomers, the relative stability of the reactant isomers ($\Delta E_{(cis/trans)R}$) also needs to be examined; the results are given in Table 1. The relative stability $\Delta E_{(cis/trans)R}$ is 4.2, 3.8, and 0.9 kcal mol^{-1} for the Ni, Pd, and Pt complexes, respectively, when the ligand L is PH_3. The positive value of $\Delta E_{(cis/trans)R}$ means that the *trans*-reactant is more stable than the *cis*-reactant. The larger size of the central metal atom (Ni < Pd < Pt) is reflected in the decreased value of $\Delta E_{(cis/trans)R}$. The *cis*-isomer is as stable as the *trans*-isomer when the central metal is Pt, and both reactant isomers are expected to be involved to a similar extent in the reaction. The

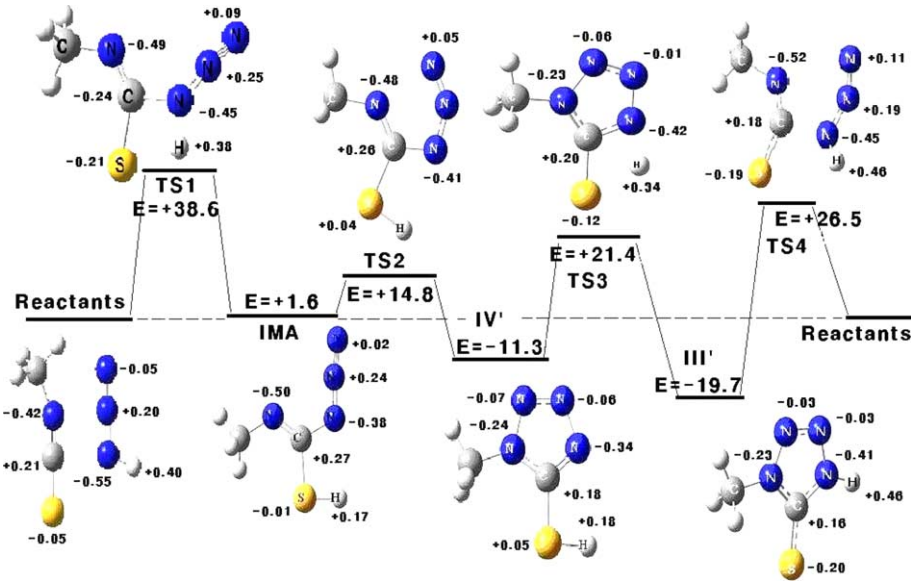

Fig. 1. The relative energies, optimized structures, and atomic partial charges of reactants, product isomers, transition states, and an intermediate of the reaction between methyl isothiocyanate and hydrazoic acid.

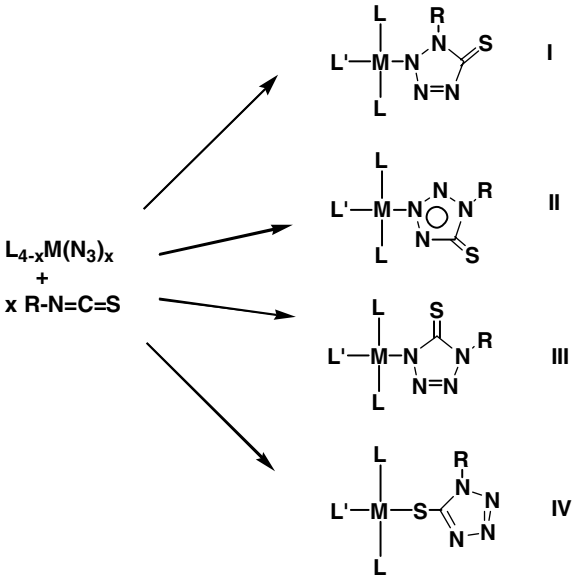

Scheme 1.

$\Delta E_{(cis/trans)R}$ values increase to 8.1, 6.0, and 4.0 kcal mol^{-1} when the ligand L is PMe_3, which reflects the larger size of PMe_3 compared to PH_3.

Although none of the *cis*-product isomer is actually calculated, we expect that the $\Delta E_{(cis/trans)}$ value of the product will become much larger than the corresponding value of the reactant because the small azide group (N_3) is replaced by much larger groups, either an N-coordinated tetrazolato (**I**, **II**, and **III**) or an S-coordinated tetrazole-thiolato (**IV**) ligand. The large $\Delta E_{(cis/trans)}$ values of the products provide a quantitative basis for why only *trans*-isomer products are actually synthesized, although the result can easily be predicted qualitatively just based on the basic chemical concept of steric hindrance.

According to the calculated reaction energies with L = PH_3 and R = CH_2CH_3 (Table 1), the formation of **I** is endothermic for all cases with reaction energies of 10.3, 9.3, and 10.6 kcal mol^{-1} for M = Ni, Pd, and Pt, respectively. This implies that the N-coordinated product **I** is thermodynamically unstable and thus unlikely to form. The same endothermic characteristic is also observed in the reactions of trialkyl tin azides (14.2 and 6.9 kcal mol^{-1}) and hydrazoic acid (5.5 kcal mol^{-1}).

The optimized geometry of the product shows that the five-member ring of **I** deviates noticeably from a planar structure. The C-atom of the R group makes a *gauche*-like conformation with respect to M (the metal atom of metal-azido complexes or the H-atom of hydrazoic acid) along the N–N bond. On the other hand, the tetrazole ring has an almost perfect planar structure in the other three product isomers, **II**, **III**, and **IV**. The S-atom as well as the C-atom of the R group are also located on the same plane of the ring.

The formation of isomer **II** turns out to be exothermic; the reaction energies are −17.7, −18.2, and −22.6 kcal mol^{-1} for M = Ni, Pd, and Pt, respectively. The reaction energies are 5.2 and −4.1 kcal mol^{-1} for the tin azide cases and −3.8 kcal mol^{-1} for the hydrazoic acid case. The magnitudes of the exothermic reaction energies are much smaller than the reaction energies for the formation of either **III** or **IV**.

All of the reactions that form **III** and **IV** are highly exothermic, with the reaction energy ranging from −50.9 to −61.6 kcal mol^{-1} for M = Ni, Pd, and Pt. The values are still large, ranging from −45.5 to −57.8 kcal mol^{-1}, even when the ligand L is changed

from PH_3 to PMe_3. The reaction energy magnitudes for **III** and **IV** for the tin azide and hydrazoic acid cases also increased noticeably from the reaction energy of isomer **II**. The reaction energies imply that the main product will be either the **III** (N-coordinated tetrazolato) or the **IV** (S-coordinated tetrazole-thiolato) isomer.

The relative energies of the **III** and **IV** isomers, ΔE_{Rel}, are also given in Table 1. The positive value of ΔE_{Rel} implies that **III** is more stable than **IV**, and it is shown that **III** is more stable than the corresponding **IV** isomer in most cases. Although the stability is reversed when the metal is Pd, the differences are very small (-3.1 and -0.1 kcal mol^{-1}).

To provide greater insight into the effect of the ligand L and alkyl group R, the reaction energy is calculated for different cases of two ligands ($L = PH_3$ and PMe_3) and four alkyl groups ($R = H$, CH_3, CH_2CH_3, $CHCH_2$, and C_6H_5), as collated in Table 2. The first noticeable feature is that the sign of ΔE_{Rel} is positive in most cases, reflecting the fact that the **III** isomer is more stable than the corresponding **IV** isomer, except for the case where $L = PH_3$ and $M = Pd$. The result is in agreement with the expectation that the main product of this reaction will be the N-coordinated tetrazole **III** [9–11]. The second significant feature of the data is that the relative energy does not depend much on alkyl group R, especially for $L = PH_3$. When $L = PMe_3$, the replacement of $R = H$ with $R = CH_3$ causes a decrease in ΔE_{Rel}, but further change of the alkyl group causes little change in the relative energy.

The main conclusion from the results in Tables 1 and 2 is that the relative stability between two possible product isomers, N-coordinated tetrazole (**III**) and S-coordinated tetrazole-thiolato (**IV**) products, is in accordance with the expectation that the N-coordinated tetrazole (**III**) isomer will be the main product. This conclusion, however, stands in contrast to a recent experimental finding that only the S-coordinated tetrazole-thiolato (**IV**) is actually synthesized [13,14]. It is now clear that the relative stability of product isomers cannot explain the experimental result, and a more detailed study of the reaction mechanism is necessary.

3.2. The reaction between methyl isothiocyanates and hydrazoic acid

Before studying our target reaction, the reaction of organic isothiocyanates with metal-azido complexes, the reaction of methyl isothiocyanate with hydrazoic acid was studied, because it is much simpler and is expected to provide some basic insights concerning the mechanism of our target reaction. The reaction of methyl isothiocyanates and hydrazoic acid can produce two major products, **III′** and **IV′**, shown in Scheme 2.

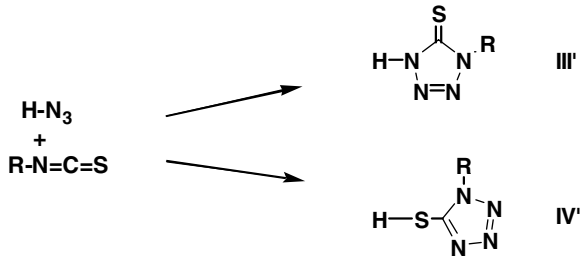

Scheme 2.

The structures of the intermediate (hereafter IMA), two product isomers (**III′** and **IV′**), and four transition structures (**TS1**, **TS2**, **TS**, and **TS4**) along the reaction path are obtained by using the B3LYP/6-31G(d) method. The relative energy and some selected bond lengths and angles of the structures as well as the lowest vibrational frequency of each structure are collated in Table 3. The reliability of each transition structure is supported by only one negative vibrational frequency of the structure, whereas that of the stationary structure of an intermediate or a product is manifest from the positive calculated frequencies.

To check the reliability of the results with the 6-31G(d) basis, all of the properties are calculated again by using very large basis sets, the 6-311++G(2d,p) [21]; the results obtained using the B3LYP/6-311++G(2d,p) method are given in parentheses in Table 3. Although the calculated values are changed slightly by increasing the basis set size, the changes are small enough that they should not affect our analysis of the reactions. Thus, hereafter our discussion will be based on the results obtained using the 6-31G(d) basis set, because the 6-311++G(2d,p) basis set is too large for the study of the target reactions discussed in the next section.

The optimized structures and relative energies of the IMA, two product isomers (**III′** and **IV′**), and four transition structures with respect to separated reactants are depicted in Fig. 1. To provide some qualitative insight into the impetus of the reaction steps, the partial atomic charges, calculated by using the natural bond orbital analysis method [22], are also included in the figure. In conjunction with the IRC optimization technique [23], we have confirmed that the forward and backward optimizations of each transition structure do generate one of the products, reactants, or intermediates on both sides of the transition structure.

Fig. 1 shows that the **III′** isomer is more stable than the **IV′** isomer, as mentioned in the discussion of the data in Table 1. Compound **III′** is produced in a single step, whereas **IV′** in two steps. The reaction barrier to generate **III′**, the activation energy to **TS4**, is also smaller than that for **IV′**, the activation energy to **TS1** (26.5 kcal mol^{-1} versus 38.6 kcal mol^{-1}). The activation barrier magnitudes are comparable to those observed in the reaction mechanism of tetrazole formation by the addition of azide to nitriles, in which the barrier is

31.6 kcal mol^{-1} without catalyst and 26.3 (19.1) kcal mol^{-1} with $ZnBr_2$ ($AlCl_3$) as catalyst [7].

The changes in bond lengths and atomic partial charges of reactants, transition states, and products along the reaction paths, shown in Fig. 1 and Table 3, provide us with a qualitative explanation of the reaction. The large negative partial charge of the first N-atom of hydrazoic acid is the main impetus of the reaction toward both **TS1** and **TS4**. Once the azide N-atom makes a nucleophilic attack to the C-atom of the isothiocyanate group, the reaction proceeds through **TS1** and generates the imidoyl azide intermediate, IMA. **TS1** is attained by the involvement of the S-atom in addition to the nucleophilic attack; its involvement leads to the formation of a bond between S and H in the IMA. The change in geometry as well as the atomic partial charges from IMA to **TS2**, on the other hand, shows that the **TS2** structure is attained mainly by an electrophilic attack of the terminal N-atom of the azide moiety toward the N-atom of the isothiocyanate. The tetrazole ring is almost completed at **TS2**, and the final product **IV**′ is formed upon ring closure. The activation energy of this step, about 13 kcal mol^{-1}, is reasonably small.

In contrast to the above two-step reaction, **III**′ can be produced by a single-step reaction through **TS4**. Both nucleophilic attack of the negatively charged N-atom and electrophilic attack of the positively charged terminal N-atom of the azide, toward the C- and the N-atom of isothiocyanate, respectively, take place simultaneously in the formation of **TS4**. The S-atom of the isothiocyanate is not involved in the formation of **TS4**, in contrast to the formation of **TS1**, which involves the S-atom. Detailed values of important bond lengths and angles of **TS4** are included in Table 3. The N–N–N bond of the azide is already bent slightly toward the N-atom of the isothiocyanate: $\angle_{N\text{–}N\text{–}N} = 148.1°$. The S–C–N–C isothiocyanate backbone is also deformed sufficiently to mimic the moiety in the final product **III**′. Product **III**′ is produced upon ring closure from **TS4** without requiring migration of the H-atom. This reaction path is very similar to the concerted [2 + 3] addition of an organic azide (R–N_3) and an organic nitrile (R–CN) [6b,16].

Fig. 2 provides further insight into the differences related to **TS1** and **TS4**. The side and the plan views of **TS4** at the top and the bottom of Fig. 2, respectively, show that the overall structure is close to planar, which is also indicated by the dihedral angle of the plane: $\angle_{N3\text{–}N1\text{–}C\text{–}N4} = 9.1°$. The pseudo-planar structure is in accordance with the concerted [2 + 3] addition. The H-atom of the hydrazoic acid is not involved in the formation of **TS4**, and is located slightly away from the plane: $\angle_{H\text{–}N1\text{–}C\text{–}S} = 25.3°$. On the other hand, the H-atom of hydrazoic acid in **TS1** makes a plane with the S-atom that participates in the formation of the structure: $\angle_{H\text{–}N1\text{–}C\text{–}S} = 5.1°$. Meanwhile, the azide moiety of **TS1**

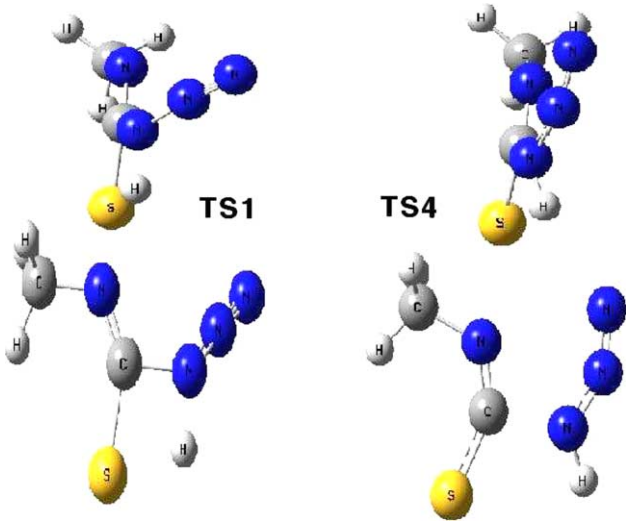

Fig. 2. The side and plan views, from top to bottom respectively, of TS1 and TS4.

deviates from the five-member ring conformation: $\angle_{N3\text{–}N1\text{–}C\text{–}N4} = -46.9°$. The side and plan views of **TS1** explain the difficulty of ring closure to tetrazole directly from **TS1**.

As a summary of the comparison between **TS1** and **TS4**, the nucleophilic attack of the negatively charged first N-atom of hydrazoic acid is the common factor of the two reaction paths – the two-step reaction for **IV**′ and the single-step reaction for **III**′. The electrophilic attack of the positively charged terminal N-atom of hydrazoic acid, in addition to the above nucleophilic attack, makes the concerted [2 + 3] addition toward **TS4** and product **III**′. On the other hand, the involvement of the S-atom of isothiocyanate directs the reaction toward **TS1** followed by the production of **IV**′ through **TS2** by the second step of electrophilic attack of the terminal N-atom.

The transition structure between the two product isomers, **TS3**, corresponds to the saddle point in the migration of a proton from the S- to the N-atom. The energy of **TS3** is 21.4 kcal mol^{-1} higher than initial reactant. The main impetus of the movement is the positively charged proton and the negative partial charge of the N-atom (N_1 in Table 3). Once **IV**′ is produced through the left-side reaction steps (reactants → **TS1** → IMA → **TS2**) of Fig. 1, product **IV**′ has to overcome the activation barrier of 32.7 kcal mol^{-1} in order to generate isomer **III**′, the thermodynamically more stable structure. On the other hand, the activation barrier for the migration of the proton becomes 41.1 kcal mol^{-1} when **III**′ is produced by the single step through **TS4**, which is somewhat larger than the activation barrier from **IV**′ to **III**′.

The above results imply that the production of **III**′ is more favorable, both kinetically and thermodynamically, over the production of **IV**′. Compound **III**′ has

been synthesized [24], whereas the synthesis of **IV′** has not yet been reported.

3.3. The reaction of methyl isothiocyanate with trimethyl tin azide and azido triphosphine metal(II) cation

Two azido ligands of the di(azido)bis(phosphine) metal complex are replaced by two tetrazole (or thiotetrazole) groups in the reaction with two isothiocyanate molecules, as shown in Scheme 1. The replacement can proceed either in a concerted manner, at both sides simultaneously, or sequentially, one side then the other in a stepwise manner. Direct theoretical study of the transition structure is prohibitively complicated due to the reactions at both sides as well as the large number of degrees of freedoms of the reactants and products involved. To reduce the computational complexity without loss of essential features, we studied the model reaction of azido tris(phosphine) metal(II) complex cation for Pt(II) and Pd(II) with one methyl isothiocyanate molecule, as shown in Scheme 3. Although the possible

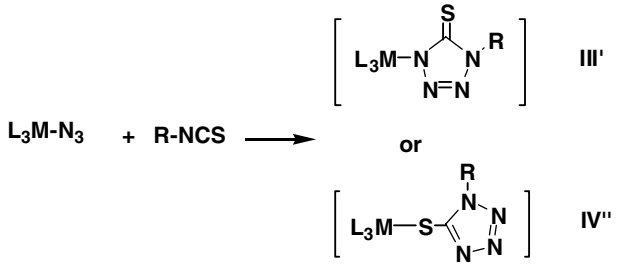

Scheme 3.

trans-effect of the ligand on the reaction mechanism cannot be accounted for by the model reaction, the main features of our target reactions are expected to be disclosed.

The reaction of methyl isothiocyanate (R-NCS) with trimethyl tin azide is also reported in this section because it is a prototype for many reactions studied in the earlier experiment [13], and turns out to follow a very similar reaction path to the above model reaction.

The main results of the energetic relationship among reactants, product isomers, an intermediate, and transition structures, obtained by the B3LYP/6-31G* method, are depicted in Fig. 3 for the cases where M = Pt. Selected bond lengths, angles, and the lowest vibrational frequency are also collated in Table 4. All of the corresponding results for M = Pd or M = Sn were also obtained by the B3LYP/6-31G* method. The numbers in parentheses and brackets in Fig. 3 and Table 4 correspond to the cases of M = Pd and M = Sn, respectively. In order to emphasize the similarity among the four reactions represented in Figs. 1 and 3, the changes in partial atomic charge of some selected atoms directly related to either the nucleophilic or electrophilic attack are collated in Table 5.

In spite of numerous attempts to find possible transition structures of the reactions with activation energy below ~50 kcal mol^{-1}, only one transition structure was located, regardless of whether **III″** or **IV″** was an expected product. The first transition structure, **TS1** in Fig. 3, is very close to the **TS1** in Fig. 1. The structure corresponds to the result of the S-atom approaching the metal atom and the partial dissociation of the bond

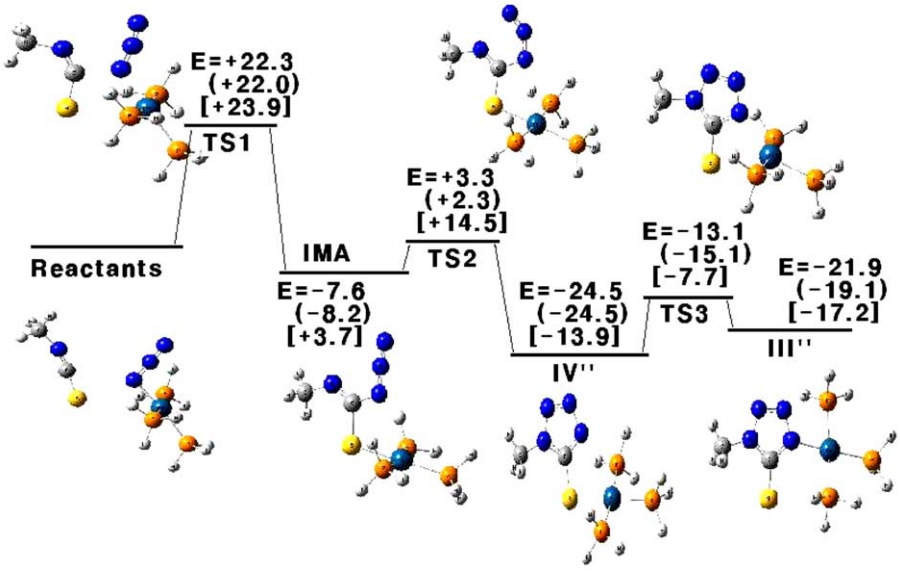

Fig. 3. The relative energies and optimized structures of reactants, product isomers, transition states, and an intermediate of the reaction between methyl isothiocyanate and azido tris(phosphine) Pt(II) complex. The relative energies of the cases with azido tris(phosphine) Pd(II) complex and trimethyl tin compound are given in parentheses and brackets, respectively.

Table 5
The change in partial atomic charges of reactants, transition structures, and the intermediate along the reaction path in Figs. 1 and 3 for M = H, Pt(II), and Sn

	M	C1	N1	N3	N4
Reactants	H	+0.21	−0.55	−0.05	−0.42
	Pt	+0.21	−0.58	−0.07	−0.42
	Sn	+0.21	−0.73	−0.15	−0.42
TS1	H	−0.24	−0.45	+0.09	−0.49
	Pt	+0.23	−0.55	+0.04	−0.48
	Sn	−0.22	−0.63	−0.01	−0.51
IMA	H	+0.27	−0.38	+0.02	−0.50
	Pt	+0.26	−0.45	+0.05	−0.48
	Sn	+0.28	−0.42	+0.01	−0.51
TS2	H	+0.25	−0.41	+0.05	−0.48
	Pt	+0.26	−0.46	+0.09	−0.46
	Sn	+0.28	−0.46	+0.05	−0.49

The order of atoms is shown in Tables 3 and 4.

between the metal atom and the coordinated N-atom of the azido group. The central metal atom and the coordinated N-atom of the azido moiety adjust to make a coplanar alignment with the SCN-R part of the isothiocyanate. The SCN-R backbone is also bent noticeably. The activation energy of **TS1** is 22.3 (22.0) [23.9] kcal mol^{-1} for M = Pt (Pd) [Sn], which is about 15 kcal mol^{-1} lower than the corresponding activation barrier in the reaction of the isothiocyanate with hydrazoic acid, 38.6 kcal mol^{-1} in Fig. 1.

The forward optimization of **TS1** produced neither **III**″ nor **IV**″, but a new intermediate (IMA) structure with all positive vibrational frequencies, confirming that it is a true stationary structure. The IMA structure in Fig. 3 is also very close to the IMA in Fig. 1. The intermediate of imidoyl azide (R–N = C(SR′)–N_3) form corresponds to the intermediate discussed in Section 3.2 for the reaction with hydrazoic acid. The IMA energy is −7.6 (−8.2) [+3.7] kcal mol^{-1} with respect to the separated reactants when M = Pt (Pd) [Sn]. The main impetus of the first step from reactants to the IMA via **TS1** is the nucleophilic attack of the coordinated N-atom of the azido moiety toward the C-atom of the isothiocyanate, as reported in Section 3.2. The similarity is also clear from the fact that the atomic partial charges in Table 5 are largely independent of the identity of M. The approach of the S-atom toward the central metal, which corresponds to the involvement of the S-atom in the formation of **TS1** described in Section 3.2, is also an indispensable factor. The overall process of the first step, which is also the most crucial step of all the reaction steps below, corresponds to the approach of the S-atom toward the central metal and the concerted nucleophilic attack of the coordinated N-atom of the azido group towards the C-atom of isothiocyanate. The IMA structure shares features with the imidoyl azide intermediate previously found in the theoretical study on the mechanism of addition of azide to nitriles [6].

The second transition structure, **TS2**, connects the intermediate to the product isomer **IV**″. We have confirmed that the forward and the backward geometry optimization of **TS2** produces the intermediate and the **IV**″ product, respectively. The relative energy of **TS2** is only +3.3 (+2.3) [+14.5] kcal mol^{-1} and the activation of the second step from the intermediate corresponds to 10.9 (10.5) [10.8] kcal mol^{-1} when M = Pt (Pd) [Sn]. The change of atomic partial charges in Table 5 shows that the main change of the second step is the ring closure by the electrophilic attack of terminal N-atom of the azido ligand to the N-atom of isothiocyanate part, the same as in the previous section.

The third reaction step corresponds to the isomerization between the **IV**″ and **III**′ products, and the transition structure, **TS3**, is located at the midpoint on the pathway of metal migration from S to N, or vice versa. The main impetus of the isomerization is the migration of the positively charged central metal from the S-atom to the negatively charged N-atom, N_1 in the structure depicted in Tables 4 and 5. The activation energy from **IV**″ to **TS3** is 11.4 (9.4) [6.2] kcal mol^{-1} for M = Pt (Pd) [Sn], which can be compared with the corresponding value, 8.8 (4.0) [9.5] kcal mol^{-1}, for the reverse of this step, from **III**″ to **TS3**. The activation energies, 4.0–11.4 kcal mol^{-1}, are noticeably smaller than those between **III**′ and **IV**′ of Fig. 1 (32.7–41.1 kcal mol^{-1}). The larger size of the metals compared with the proton of the hydrazoic acid is the main reason for the drastic decrease in the activation energy. The activation barrier for the actual experiment [14], however, is expected to be higher than that for our model reactions due to increased steric hindrance and decreased atomic partial charges.

One point that we must note here is the change of relative stability of ΔE_{Rel} compared with those of Table 1. Product **III** is more stable than **IV** when the metal moiety M has two phosphine ligands, as in the cases in Table 1 and Fig. 1, but the relative stability is reversed when the M moiety has three phosphine ligands. The *trans*-effect is therefore neglected due to the replacement of one azido group at the *trans*-position of reactants with the phosphine ligand. The change of total charge, from neutral to positive by the replacement of one azido ligand with PH_3 in our model reaction, could be another reason for the reversed relative stability. Considering the reversed relative stability, the activation energy from the N-coordinated tetrazole to **TS3** is expected to be larger than the activation energy from the S-coordinated tetrazole-thiolato to **TS3** in actual reactions with di(azido)bis(phosphine) metal complexes of Pd(II) and Pt(II) [14].

3.4. The reaction with the Ni(II) complex

We carried out a study very similar to those described in Section 3.3 in order to find the corresponding transition structures for Ni(II) complexes. We did not, however, observe the formation of a transition structure similar to those of the Pt(II) and Pd(II) cases; instead, we found that one PH_3 ligand dissociates when the S-atom of isothiocyanate approaches the central Ni atom. Numerous attempts with many different techniques consistently produced this dissociation. The theoretical result is partially in accordance with the experimental result that no product is actually identified when the central metal is Ni(II) [14]. This result merits further study with more elaborate theoretical methods, including solvent effects and simultaneous replacement of two azido groups at both sides of the central metal atom. The detailed reaction mechanism of the Ni(II) complex remains an open question.

4. Conclusions

In spite of increasing interest in the possibility that the reaction between organic isothiocyanates and metal-azido complexes is a promising alternative source of tetrazoles, the reaction mechanism has not previously been studied in detail, either theoretically or experimentally. Our theoretical study shows that the relative stability between two possible product isomers (S-coordinated tetrazole-thiolato and N-coordinated tetrazolato compounds) of the reaction is in accordance with previous expectations [6–11], but stands in contrast to recent experimental results [13,14]. To resolve the conflicting results and to provide detailed insights, the reaction mechanisms of methyl isothiocyanate with hydrazoic acid, azido tris(phosphine) transition metal cationic complexes, and trimethyl tin azide were studied. In spite of the quite different nature of the three azides, our study disclosed the following common features.

The overall reaction mechanism is composed of three reaction steps, regardless of the identity of the central metal. The first step corresponds to the approach of the isothiocyanate S-atom to the central metal atom and the concerted nucleophilic attack of the coordinated azido N-atom to the isothiocyanate C-atom. The activation energy of the first transition structure, **TS1**, is 22–24 kcal mol^{-1}. **TS1** transforms to an intermediate having the imidoyl azide (R–N=C(SR′)–N_3) form, which was found in an earlier theoretical study on the mechanism of tetrazole formation by addition of azide to nitriles [6]. This intermediate becomes a S-coordinated tetrazole-thiolato structure, **TS2**, during the second reaction step. The main impetus of the second step is the electrophilic attack by the azido terminal N-atom to the isothiocyanate N-atom in the intermediate. The activation energy from the intermediate to **TS2** is about 11 kcal mol^{-1}. The N-coordinated tetrazole could be made from the S-coordinated tetrazole-thiolato product only after isomerization during the third reaction step, in which the central metal atom migrates from the S- to the N-atom. The N-coordinated tetrazole, however, has not yet been synthesized, except for the reactions with hydrazoic acid or azide salt.

A single-step mechanism to the N-coordinated tetrazole is also observed when the azide is hydrazoic acid. The single step corresponds to the concerted [2 + 3] addition mechanism, and is favored over the above three-step mechanism, both kinetically and thermodynamically, in the case with hydrazoic acid. The single-step mechanism, however, is not observed with metal-azido complexes. The main reason is the high affinity of the isothiocyanate S-atom to metal atoms, which leads preferentially to **TS1** (Figs. 1 and 3) of the three-step mechanism rather than to **TS4** (Fig. 1) of the single-step mechanism. The activation barrier to **TS1** is also lowered substantially by the affinity between the S-atom and the central metal.

Acknowledgement

This work is supported by Korea Science and Engineering Foundation Grant R05-2004-000-10995-0.

References

[1] D. Moderhack, J. Prakt. Chem. 340 (1988) 687–709.
[2] H. Singh, A.S. Chawla, V.K. Kapoor, D. Paul, R.K. Malhotra, Prog. Med. Chem. 17 (1980) 151–183.
[3] M. Hiskey, D.E. Chavez, D.L. Naud, S.F. Son, H.L. Berghout, C.A. Bome, Proc. Int. Pyrotech. Semin. 27 (2000) 3–14.
[4] G.I. Koldobskii, V.A. Ostrovskii, Usp. Khim. 63 (1994) 847–865.
[5] (a) S. Kertit, B. Hammouti, App. Sur. Sci. 93 (1996) 59–66;
(b) E. Szöcs, I. Bakó, T. Kosztolányi, I. Bertóti, E. Kálmán, Elctrochem. Acta 49 (2004) 1371–1378.
[6] (a) R.N. Butler, in: A.R. Katritzky, C.W. Rees, E.F.V. Scriven (Eds.), Comprehensive Heterocyclic Chemistry, vol. 4, Pergammon, Oxford, UK, 1996;
(b) Z.P. Demko, K.B. Sharpless, Angew. Chem., Int. Ed. 12 (2002) 2113–2116.
[7] (a) F. Himo, Z.P. Demko, L. Noodleman, K.B. Sharpless, J. Am. Chem. Soc. 124 (2002) 12210–12216;
(b) F. Himo, Z.P. Demko, L. Noodleman, K.B. Sharpless, J. Am. Chem. Soc. 125 (2003) 9983–9987.
[8] (a) J. Beck, J. Organomet. Chem. 383 (1990) 143;
(b) L. Busetto, A. Palazzi, R. Ros, Inorg. Chim. Acta 13 (1975) 233;
(c) Z.P. Demko, K.B. Sharpless, J. Org. Chem. 66 (2001) 7945–7950.
[9] (a) P. Paul, K. Nag, Inorg. Chem. 26 (1987) 2969;
(b) R. Das, P. Paul, K. Nag, Venkatsubramanian, Inorg. Chim. Acta 182 (1991) 221.
[10] P. Kreutzer, Ch. Weis, H. Bock, J. Erbe, W. Beck, Chem. Ber. 116 (1983) 2691.

[11] F. Sato, M. Etoh, M. Sato, J. Organomet. Chem. 70 (1974) 101.
[12] P. Dunn, D. Oldfield, Aust. J. Chem. 24 (1971) 645.
[13] R.J. Deeth, K.C. Molloy, M.F. Mahon, S. Whittaker, J. Organomet. Chem. 430 (1992) 25–35.
[14] (a) Y.-J. Kim, J.-T. Han, S. Kang, W.S. Han, S.W. Lee, Dalton Trans. (2003) 3357–3366;
(b) Y.-J. Kim, X. Chang, J.-T. Han, M.-S. Lim, S.W. Lee, Dalton Trans. (2004) 3699–3708.
[15] (a) W.G. Finnegan, R.A. Henry, R. Lofquist, J. Am. Chem. Soc. 80 (1958) 3908–3911;
(b) E. Jursic, Z. Zdravkovski, Theochem 118 (1994) 11.
[16] (a) R. Huisgen, J. Org. Chem. 33 (1968) 2291–2297;
(b) V.A. Ostrovskii, V.S. Poplavski, G.I. Koldobskii, G.B. Erusalimskii, Khim. Geterotsikl. Soedin. 9 (1992) 1214.
[17] (a) A.D. Becke, Phys. Rev. A 38 (1988) 3098–3100;
(b) A.D. Becke, J. Chem. Phys. 98 (1993) 5652–5684.
[18] M.J. Frisch, G.W. Trucks, H.B. Schlegel, G.E. Scuseria, M.A. Robb, J.R. Cheeseman, J.A. Montgomery Jr., T. Vreven, K.N. Kudin, J.C. Burant, J.M. Millam, S.S. Iyengar, J. Tomasi, V. Barone, B. Mennucci, M. Cossi, G. Scalmani, N. Rega, G.A. Petersson, H. Nakatsuji, M. Hada, M. Ehara, K. Toyota, R. Fukuda, J. Hasegawa, M. Ishida, T. Nakajima, Y. Honda, O. Kitao, H. Nakai, M. Klene, X. Li, J.E. Knox, H.P. Hratchian, J.B. Cross, C. Adamo, J. Jaramillo, R. Gomperts, R.E. Stratmann, O. Yazyev, A.J. Austin, R. Cammi, C. Pomelli, J.W. Ochterski, P.Y. Ayala, K. Morokuma, G.A. Voth, P. Salvador, J.J. Dannenberg, V.G. Zakrzewski, S. Dapprich, A.D. Daniels, M.C. Strain, O. Farkas, D.K. Malick, A.D. Rabuck, K. Raghavachari, J.B. Foresman, J.V. Ortiz, Q. Cui, A.G. Baboul, S. Clifford, J. Cioslowski, B.B. Stefanov, G. Liu, A. Liashenko, P. Piskorz, I. Komaromi, R.L. Martin, D.J. Fox, T. Keith, M.A. Al-Laham, C.Y. Peng, A. Nanayakkara, M. Challacombe, P.M.W. Gill, B. Johnson, Chen, M.W. Wong, C. Gonzalez, J.A. Pople, Gaussian 03, Revision B.04, Gaussian, Inc., Pittsburgh, PA, 2003.
[19] (a) P.C. Hariharan, J.A. Pople, Theor. Chim. Acta 28 (1973) 213;
(b) M.M. Francl, W.J. Pietro, W.J. Hehre, J.S. Binkley, M.S. Gordon, D.J. DeFrees, J.A. Pople, J. Chem. Phys. 77 (1982) 3654.
[20] (a) P.J. Hay, W.R. Wadt, J. Chem. Phys. 82 (1985) 270;
(b) P.J. Hay, W.R. Wadt, J. Chem. Phys. 82 (1985) 299.
[21] (a) A.D. McLean, G.S. Chandler, J. Chem. Phys. 72 (1980) 5639;
(b) R. Krishnan, J.S. Binkley, R. Seeger, J.A. Pople, J. Chem. Phys. 72 (1980) 650;
(c) T. Clark, J. Chandrasekhar, G.W. Spitznagel, P.V.R. Schleyer, J. Comp. Chem. 4 (1983) 294.
[22] E.D. Glendening, A.E. Reed, J.E. Carpenter, Weinhold, F. NBO Version 3.1.
[23] (a) G. Gonzalez, H.B. Schlegel, J. Chem. Phys. 90 (1989) 2154;
(b) G. Gonzalez, H.B. Schlegel, J. Phys. Chem. 94 (1990) 5523.
[24] E. Lieber, Raamachandran, Can. J. Chem. 37 (1959) 101.